Fiberboard Made from Scrap Denim: Characterization of its Properties by Effective Bulk Modulus Elastography

Sheldon Q. Shi,[a,*] Zhiying Cui,[a] Yuqi Jin,[a] Lee Smith,[a] H. Felix Wu,[b] and Arup Neogi [c]

Fiberboards from scrap denim were fabricated using two different resins, melamine urea formaldehyde (MUF) and polymeric methylene diphenyl diisocyanate (pMDI). Resin content and MUF-pMDI weight ratio were studied. Physical and mechanical tests determined the modulus of elasticity (MOE), modulus of rupture (MOR), internal bond (IB), thickness swell (TS), and water absorption (WA). The resin content had significant impact on all properties. The MOE and IB were affected by the MUF-pMDI ratio. With 17 wt% more pMDI resin portion in the core layer of the denim boards, the IB for the denim fiberboard with a resin content of 15% was enhanced by 306%, while by 205% for the resin content of 25%. The increase in pMDI portion in the core layer of the boards improved both TS and WA of the scrap denim fiberboard. Effective bulk modulus elastography (EBME) was used to measure the acoustic reflection for the estimation of the strength properties of the denim fiberboard. The modulus results from EBME were correlated to the MOR, MOE, and IB of the denim fiberboard. A high correlation was found between the modulus from EBME and IB ($R^2 > 0.98$). EBME can be a great technique to evaluate the bulk modulus distribution of the composites.

DOI: 10.15376/biores.18.2.3279-3294

Keywords: Denim; Fiberboard; Acoustic; Effective bulk modulus elastography (EBME)

*Contact information: a: Department of Mechanical Engineering, University of North Texas, 3940 North Elm St., F101P, Denton, Texas 76207-7102 USA; b: U.S. Department of Energy, USA; c: Institute of Fundamental and Frontier Sciences, University of Electronic Science and Technology of China, Chengdu, 611731, China; *Corresponding author: Sheldon.shi@unt.edu*

INTRODUCTION

Denim has been widely used in modern society because denim products are both fashionable and durable. The textile industry consumes a large quantity of water and chemicals during the production stages, significantly impacting the environment (Luiken and Bouwhuis 2015), especially for denim fabrication, as it has an indigo dye process. According to Advancing Sustainable Materials Management, in 2014, 16.22 million tons of textile waste were generated, while only 2.62 million tons (16.2% of the total waste) were recycled. Approximately 3.14 million tons of waste, 19.4% of the total, were combusted. The remaining 10.46 million tons (64.4% of the total waste) were sent to landfill (United States Environmental Protection Agency 2016). It is urgent to have an appropriate way to recycle these textile wastes. Many people in the textile industry try to reuse recycled denim fibers in clothing products. The pieces of most denim wastes are gathered and shredded in mill machines to obtain the denim fibers. However, those recycled fibers reused in weft insert yarns are mostly shorter than virgin fibers (Luiken and Bouwhuis 2015). The mechanical strength of recycled fibers is lower than that of virgin fibers.

Many attempts have been made to use agricultural plant wastes, *e.g*., kenaf, hemp, bamboo, corn, sycamore, tea leaves, peanut, palm fronds, sorghum, sunflower, pulp, walnut shell, sugarcane bagasse, rice straw, ramie, and flax, to fabricate natural fiber composites (Ndazi *et al*. 2006; Laemlasksakul 2010; Abolfazl and Ahmad 2011; Nath and Mwchahary 2012; Pirayesh *et al*. 2012; Aghakhani *et al*. 2014; Batiancela 2014; Iswanto *et al*. 2014; Li *et al*. 2014; Smith and Shi 2015; Temitope *et al*. 2015; Xia *et al*. 2015; Cheng *et al*. 2016; Klímek *et al*. 2016; Wang *et al*. 2017; Ferrández-García 2018; Li *et al*. 2018; Wang *et al*. 2020). Denim is a sturdy cotton warp-faced textile, in which the weft passes under two or more warp threads. Considered as a natural fiber mainly consisting of cotton fibers (McLoughlin *et al.* 2015), denim is yarn-dyed, mill-finished, and usually all-cotton, although considerable quantities are of a cotton-synthetic fiber mixture. Figure 1 shows the denim fibers generated from the used denim textile. The fiber is composed mostly of the long-chain carbohydrate molecule. The secondary wall thickness of cotton fibers is directly related to the fiber properties, including strength, reactivity, and dye ability. Lewin (2006) shows a computer-generated montage of a cotton fiber segment, from which a layered structure of the cotton fiber is demonstrated. The cuticle is supposed to be a scoured and bleached fiber surface. The primary wall is a thin layer that provides the fiber with structural support and protection. The secondary wall is a thick layer formed inside the primary wall with fibrillar structures, providing the fiber with rigidity and strength (Lewin 2006).

Denim fibers

Fig. 1. Denim fibers and their microstructure

Ultrasonic testing (Bhuiyan *et al*. 2018), imaging (Boni *et al*. 2018), and evaluations (Sarro and Ferreira 2019) have continuously contributed to academia (Tang *et al*. 2019), industrial (Hwang *et al*. 2019), and biomedical fields (Sigrist *et al.* 2017). Ultrasound-based techniques provide information such as reflection intensity (Taheri and Hassan 2019) and speed of sound (Minh *et al*. 2019) to estimate discontinuity imaging and elastic properties (Reese *et al*. 2021). Ultrasonic testing techniques have been used to analyze natural fiber composites such as oriented strandboard (OSB), plywood, structural composite lumber, and fiberboard (Vun *et al*. 2003; Hsu *et al*. 2010; Sfarra *et al*. 2013). The benefit of these ultrasonic techniques is that they are non-destructive. Ultrasonic testing has been used to analyze mechanical properties, detect defects, and material grading (Sandoz 1993; Gonçalves *et al*. 2011; Yang and Yu 2017).

In the conventional acoustic inspection methods, two major divisions are applied in the industrial field. By determining the acoustic speed of sound information from the tested sample, the ultrasound non-destructive evaluation can estimate the elasticity of the sample with a pre-known value density, which is obtained usually by a pycnometer. Hence, the measured elasticity is in bulk instead of local distribution on the sample. On another side, based on the internal reflection from the tested sample, the defects and discontinuity information can be conducted based on their acoustic impedance mismatching with the surrounding materials. The examination resolution of the technique is highly connected to the operating wavelength. The target voids with a smaller size than acoustic wavelength cannot offer an additional echo.

As a combined technique, elastography provides imaging showing the elasticity variance of the materials, which has been recently developed and applied in the industrial field (Pantawane *et al.* 2021). In this study, the effective bulk modulus elastography (EBME) technique (Jin *et al*. 2019, 2020a,b; Neogi *et al*. 2020) was used to evaluate the effective bulk modulus constant between the products and their distribution in the horizontal on each plate based on measuring the acoustic impedance and effective speed of sound values. As represented by the Newton–Laplace equation, the effective bulk modulus is proportional to the density, and the study on the composite product pieces elucidated its contrast and distribution. The phase velocity is examined on the sample plates to estimate the relative homogeneity contrast along the thickness direction (Jin *et al*. 2020). Other acoustic properties are also determined, such as the coefficient of transmission, reflection, and absorption (Legendre *et al*. 2001). The acoustic properties are highly varied in composite samples due to the different processes and recipes.

The Mechanism of the EBME Technique

Effective bulk modulus elastography (EBME) is a mapping-based ultrasonic evaluation technique measuring high-frequency dynamic bulk modulus (compressive resistance) *K*. The dynamic bulk modulus carries the information on the sound velocity *c*, impedance *Z*, and density ρ using Eq. 1.

$$\boldsymbol{K = \rho c^2 = Zc} \quad (1)$$

Unlike the conventional ultrasound technique using shorter wavelength for void detection, EBME uses long wavelength estimating effective values along the depth as the effective medium theory described. The presence of the defects and discontinuity leads to a deviation in the effective bulk modulus values. The calculation of the EBME only requires the known value of the sample thickness. As shown in Fig. 2, the transducer initially emits a shout acoustic pulse propagation to the target sample with amplitude p_e (Fig. 2A). The source pulse is separated into a reflection pulse p_0 and a transmission pulse $p_e - p_0$ at the upper surface of the sample (Fig. 2B). The second reflection pulse occurs at the lower surface of the sample propagated back to the transducer with amplitude p_1 (Fig. 2C). By measuring the reflection pulses' amplitude and temporal delay, the obtained values from the experiments can be translated into the speed of sound in the sample and the acoustic impedance mismatching amount between the sample and ambient fluid. The dynamic bulk modulus can be calculated by Eq. 2,

$$\boldsymbol{K = c\, Z_0 \left(\frac{-1 - \frac{p_1}{p_e - p_0} - \sqrt{4\frac{p_1}{p_e - p_0} + 1}}{\frac{p_1}{p_e - p_0} - 2} \right)} \quad (2)$$

where $\boldsymbol{p_e}$ is the maximum absolute magnitude of the emitted pulse from the transducer, $\boldsymbol{p_0}$ and $\boldsymbol{p_1}$ are the maximum absolute magnitude of reflection from the front and back surface of the sample, $\boldsymbol{t_f}$ and $\boldsymbol{t_i}$ are the start point and endpoint of the pulse, which is determined from an automatic algorithm, $\boldsymbol{c}$ is the speed of sound in the sample, which is defined as follows,

$$\boldsymbol{c} = \frac{\boldsymbol{2d}}{\boldsymbol{t_f - t_i}} \quad (3)$$

where $\boldsymbol{d}$ is the thickness of the sample, and $\boldsymbol{Z_0}$ is the reference acoustic impedance of the ambient material (deionized water in this study).

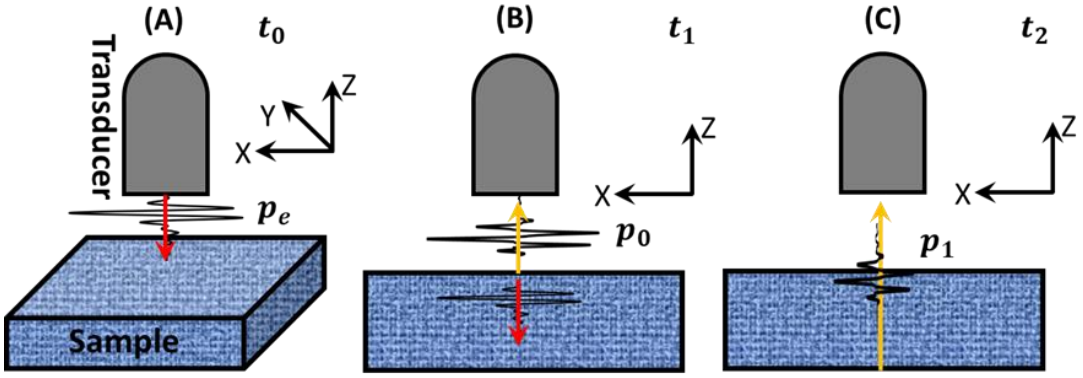

Fig. 2. Illustration of EBME measurement at three closer time points $t_0 < t_1 < t_2$

EXPERIMENTAL

Denim fibers were provided by VF Jeanwear (Greensboro, NC). These denim fibers were from the cut-outs of used denim textile generated at sawmills. Two resins were used in the fabrication of the denim fiberboard samples, polymeric methylene diphenyl diisocyanate (pMDI) resin, obtained from Huntsman LLC (Woodlands, TX), and melamine urea formaldehyde (MUF) resin, obtained from Hexion Inc. (Hope, AR).

The denim fiberboards were fabricated with three layers – top, core, and bottom-glued separately by MUF, pMDI, and MUF, respectively. Since pMDI resin tends to bond to the plates, it was used only in the core layer, while the MUF was used for the top and bottom layers. In the fabrication of a denim fiberboard, the denim fibers were put into a homemade drum blender, which a barrel rotating on a rolling device. While the blender rotated at 20 cycles/min, the resin was sprayed into the blender at a rate of 0.2 L/min. After all the resin was sprayed into the drum, the blender was kept running for another five more minutes to allow an even resin distribution. The resonated denim fibers were hand formed in a 1 ft by 1 ft forming box with a metal plate on the bottom. A release agent (Chem-Trend, Howell, MI) was sprayed on the plates evenly before forming to avoid resonated denim fibers being bonded to the metal plates. The formed resonated denim fiber mat was first cold pressed (Carver press, Dake Inc.) to reduce the mat's thickness and allow the adhesive to penetrate the fibers. The denim fiber mat was moved to a hot press to be consolidated into the final denim fiberboard. The temperature of the hot press was set to 165 °C. The pressure was set at 5 MPa, and the pressing time was 10 min. During the hot pressing, after the initial pressing, the pressure was reduced to 2.5 MPa for 1 min to allow the steam to come out of the mat to avoid the blow defect, and then increased to the target

pressure. Acetone purchased from W. M. Barr and Co., Inc. (Memphis, TN) was used to function as a release agent and clean the pMDI resin from the sprayer. Board dimension: 1 ft (length) × 1 ft (width) × 3/8 in (thickness); density: 48 pcf (0.77 g/cm^3); Equilibrium moisture content of board: 8%. The detailed experimental design is shown in Table 1. Five replicates were used for each condition.

Table 1. Experimental Design

Weight Ratio MUF: pMDI: MUF	Adhesive Content	
	15%	25%
1:1:1	Five replicates with Series No.: 15111	Five replicates with Series No.: 25111
1:2:1	Five replicates with Series No.: 15121	Five replicates with Series No.: 25121

For the 15111 and 25111 lay-ups, the thickness of each layer was 1/3 of the total board thickness. For the 15121 and 25121 lay-ups, the thickness of the top and bottom layer was ¼ of the total fiberboard thickness, while the thickness of the core was ½ of the total board thickness. After trimming the edges, the denim board sample was 11 inches by 11 inches. For each board, 2 bending specimens for modulus of electricity (MOE) and modulus of rupture (MOR) properties, 5 internal bond (IB) specimens, and 5 thickness swell (TS) and water absorption (WA) specimens were cut. All test samples were placed in a conditioning room at 65 ± 5% RH and 20 ± 3 °C for >120 h to reach their equilibrium moisture content. The moisture content of the specimens was determined according to ASTM D4442 (2016). The specific gravity (SG) was measured in accordance with the procedure described in ASTM D2395 (2017). Eight replicates were used. The physical and mechanical tests were conducted in accordance with the procedure described in ASTM D1037 (2020). For the IB testing, an Ad Tech 962 hot melt glue was used to bond the denim board specimen to the aluminum alloy blocks. The bending tests specimens were prepared to be 3 inches in width by 11 in. in length (2 in. plus 24 times the nominal thickness). Three-point bending tests were loaded at the center of span with the load applied onto the specimen's top surface. The loading speed was set at 5 mm/min with a span of 9 in. (24 times the nominal thickness). The SGs were measured from 0.84 to 0.89. A universal testing machine Shimadzu AGS-X with a maximum load of 5 kN, was used for the test.

RESULTS AND DISCUSSION

Figure 3 shows that both MOE and MOR increased as the resin content increased. The higher pMDI resin proportion (weight ratio of using MUF: MDI: MUF is 1:2:1) was used in the denim fiberboard resulted in higher the MOR and MOE values. As the resin content increased from 15% to 25%, the MOE was increased by 56.1 to 87.1%, while the MOR value increased by 128.2% for the 111 layups and by 74.9% for the 121 layups. As the resin weight ratio of MUF: pMDI: MUF increased from 1:1:1 to 1:2:1, the MOE value increased by 41.3% for 15% resin content and 17.9% for the 25% resin content, while the

MOR was increased by 71.3% at 15% resin content and by 31.2% for 25% resin content. ANOVA was conducted for the data analysis of MOE. The F values were calculated as 11.26, 61.29, and 0.10 for weight ratio, adhesive content, and interaction, respectively. In comparing with $F_{0.05,1,16} = 4.49$, it was determined that both weight ratio and resin content effects were significant, while the interaction between the two factors was not significant.

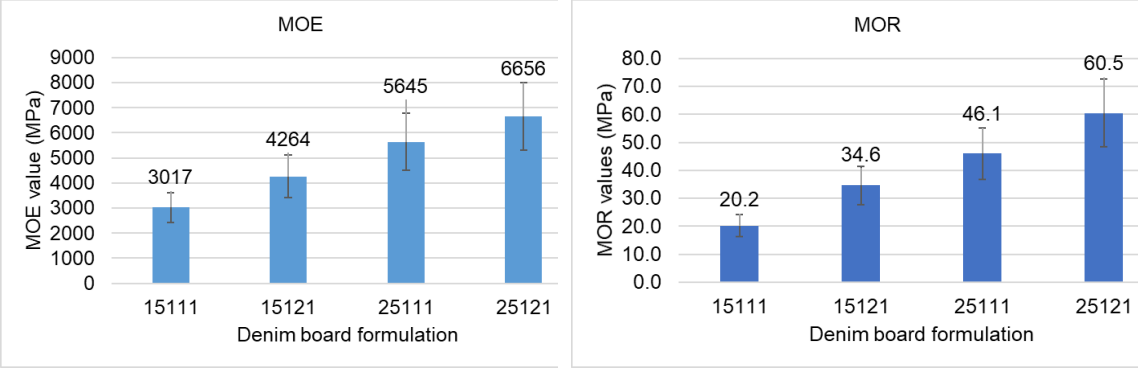

Fig. 3. Bending properties of the denim fiberboard of four different formulations

The IB strength results are shown in Fig. 4. As expected, the board with 111 layups had a relatively lower IB than that for the 121 layups. This is because less pMDI resin was used in the 111 layups. The 121 layup had 17% more pMDI in the core, while 17% less MUF was used in the top and bottom layers. However, the IB of 121 layups was 306% higher than that of 111. As the resin content was increased to 25%, the increase in IB for the board with 17% more pMDI in the core was reduced to 205%. The contribution of pMDI to the IB was more effective at lower resin content. From the ANOVA for the IB, the F values were calculated as 45.28, 3.43, and 0.0015 for weight ratio, resin content, and interaction, respectively. Compared to $F_{0.05,1,16} = 4.49$, it was determined that the weight ratio had a significant effect on the IB. In contrast, the effect of the resin content and the interaction between the resin content and weight ratio were insignificant.

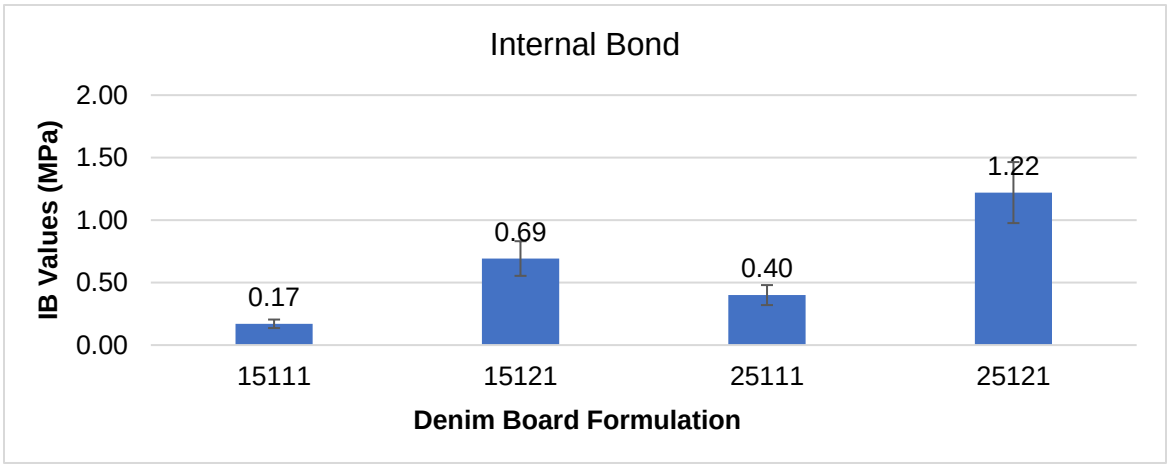

Fig. 4. Internal bond for the denim fiberboard of four different formulations

Figure 5 shows that the denim fiberboards with higher resin content had less TS and WA. The TS for the board with 25% resin content was 8.4 to 11.1%, which is lower than that with 15% resin content of 11.7 to 53.1%. However, more pMDI used in the core

would contribute to the TS. With 17 wt% more pMDI used in the core layer and 17 wt% less MUF used in the top and bottom layers, a lower TS was still obtained (9.6% for the sample 15121 compared to and 11.0% for the sample 25111). The ANOVA was conducted on the TS data, and the F values were calculated as 84.28, 56.42, and 39.49 for weight ratio, adhesive content, and interaction, respectively. Compared to $F_{0.05,1,16}$ = 4.49, the effects of MUF-pMDI weight ratio, resin content, and their interaction were all significant.

Figure 5 shows that the WA of the sample 15111 was the highest, 53.42% on average. The WA of sample 25111 was obtained as 17.06% on average, both were higher than that when the more pMDI was used in the core layer (samples 15121 and 25121). With 17 wt% more pMDI in the core layer, even though 7 wt% less MUF was used for the top and bottom layers, the average WAs were 16.49% less for sample 15121 and 11.35% less for sample 25121.

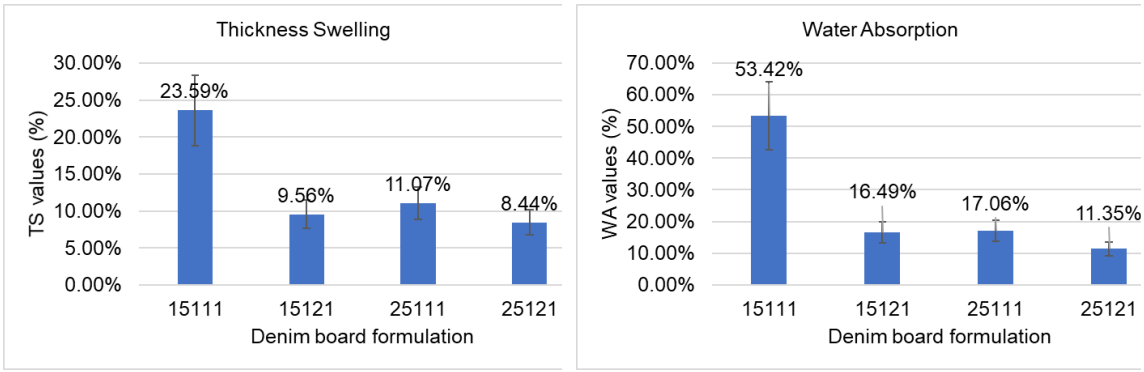

Fig. 5. Thickness swell and water absorption for the denim fiberboard of four different formulations

Both TS and WA results had a similar trend as those for the IB of the denim fiberboard, indicating that a good IB can induce a good resistance to the WA and TS. The average WA of samples 25111 and 25121 were obtained at 17.06% and 11.35%, which were 68.1% and 31.2% lower than those of samples 15111 and 15121, respectively.

The mechanical and physical properties of the denim fiberboard obtained from this study were comparable to the reported properties of the medium density fiberboard (MDF) (Mohebby *et al.* 2008). The denim fiberboard presented higher MOR (20 to 60 MPa), MOE (3,000 to 6,700 MPa), and IB (0.17 to 1.22 MPa), compared to those of MDF, 12 to 17 MPa for MOR, 1,750 to 2,100 MPa for MOE and 0.11 to 0.12 MPa for IB. The TS of denim fiberboard was in a range of 8 to 24% as compared to that of MDF (17 to 24%). The 24-hour WA was in a range of 11 to 53%, which was much less than that of the MDF (120 - 130%). The main reason for the better physical and mechanical properties of the denim fiberboard is that besides the higher denim fiber strength compared to that of the wood fiber, the resin used in this study was different, pMDI and MUF as compared to the urea formaldehyde (UF) resin used for the MDF. Also, the resin content used in this study was higher (15 to 25%) as compared to that used in the MDF (10%).

Modulus of the Denim Fiberboard Measured from EBME

Figure 6 shows the results of acoustically measured dynamic bulk modulus distribution over 4 sample plates with different recipes. Samples 15111, 15121, 25111, and 25121 were separately located in the upper left, upper right, lower left, and lower right in Fig. 6. The four samples were separated by 1 mm from each other. The red scale indicated

the linear scale dynamic bulk modulus from 0 to 7 GPa, while 0 GPa referred to the empty space between the samples. The tested areas of each sample were 40 mm by 30 mm in the scanned area. The averaged dynamic bulk modulus values of the plates with standard deviations were obtained as 3.015 ± 0.7088 GPa (15111), 4.362 ± 0.7296 GPa (15121), 3.289 ± 1.0382 GPa (25111), and 5.597 ± 0.8695 GPa (25121). The contrast of dynamic bulk modulus between the samples agreed with the previously measured static elasticity contrast. Additionally, the estimation of the elasticity variance can be important to the composite characterization, while it would be difficult to obtain from the conventional mechanical testing methods.

The lateral bulk modulus distribution is directly proportional to the effective density distribution and refers to the stability of the composition recipe and the corresponding manufacturing process. Based on the map shown in Fig. 6 and the standard deviation values, it can be concluded that samples 15111, 15121, and 25121 had better stability in terms of linear elastic incompressibility compared to Sample 25111. Sample 25111 clearly had a larger variance in distribution, which probably resulted from the poor compatibility between the composition recipe and the manufacturing process. For future manufacturing optimization, the role of dynamic bulk modulus distribution would be more significant during parametric sweep studies. To accomplish this, the horizontally averaged frequency-dependent phase velocity in the four samples along with their corresponding standard deviation were analyzed (Fig. 7).

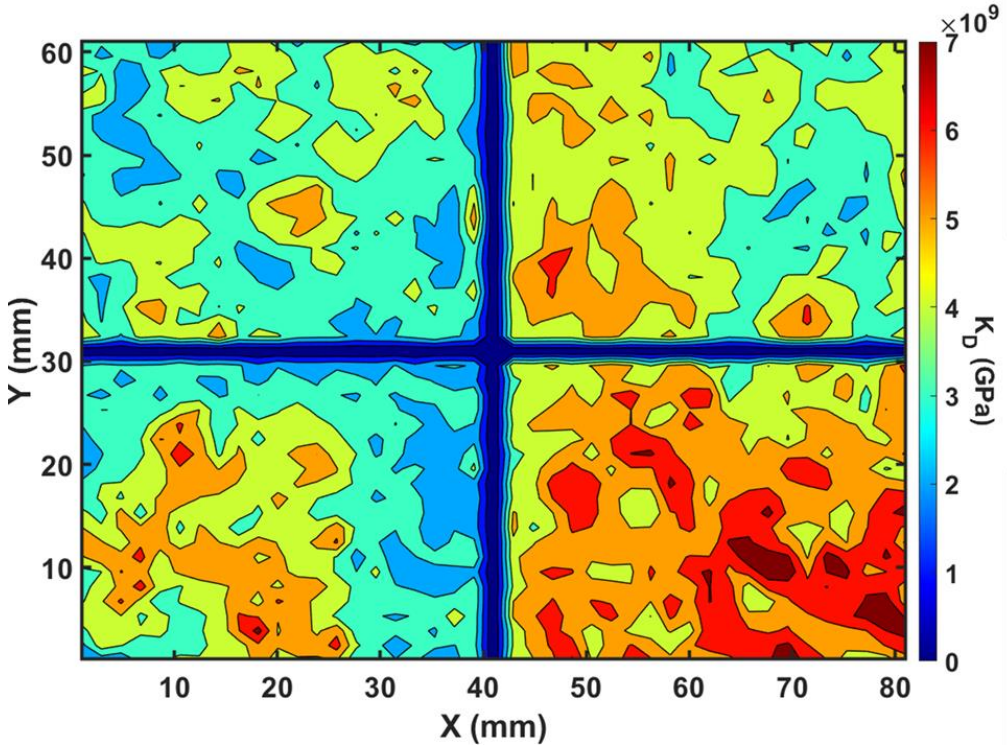

Fig. 6. Acoustic property dynamic bulk modulus distribution over four different recipes of denim fiberboard, 15111 (upper left), 15121 (upper right), 25111 (lower left), and 25121 (lower right).

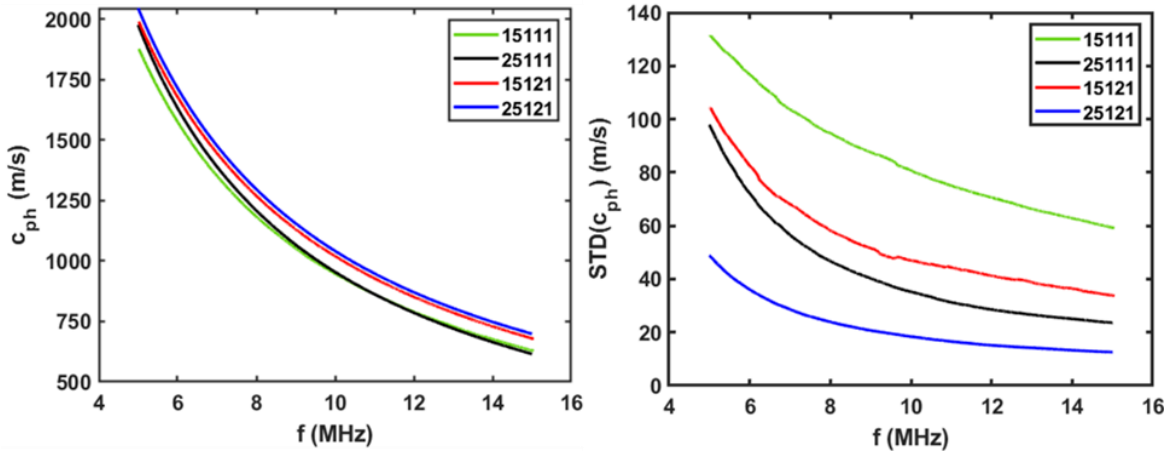

Fig. 7. Horizontally averaged frequency-dependent phase velocity for the four denim fiberboards

Over the studied frequency range, sample 25121 had the highest phase velocity in the entire pulse envelope. Samples 15121 and 15111 averaged 0.4% and 2.2% lower phase velocity compared to 25121. However, the frequency dependence of the phase velocity between those three samples was approximately identical (Fig. 7). Sample 25111 determined different frequency dependence with a larger slope. With the increase in frequency of the phase components, the phase velocity reduction amount was significantly larger than that of the other samples, indicating a larger scattering effect occurred in sample 25111 along the depth direction. The higher scattering effect in 25111 was highly possible due to the larger inhomogeneity in 25111 along the thickness direction. The right-hand curve in Fig. 7 illustrates the standard deviation of the frequency-dependent phase velocity. Similar to the averaging, the standard deviation was obtained from the horizontal array distribution. Hence, the physical representation of the standard deviation referred to the horizontal contrast of the vertical inhomogeneity along the sample plates. Sample 15111 had the highest difference on the XY plane in depth inhomogeneity. Sample 25121 still illustrated the best performance in this comparison.

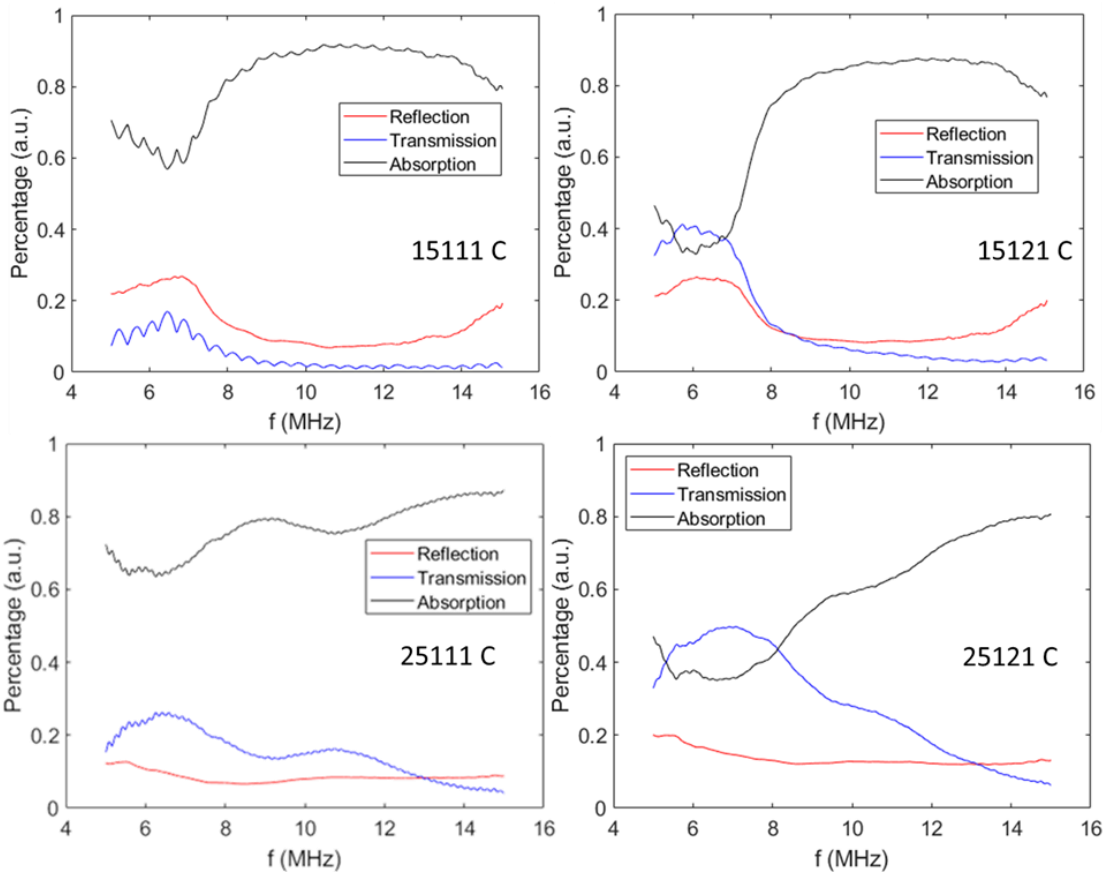

Fig. 8. Frequency-dependent averaged coefficients of reflection, transmission, and absorption over XY plane for the denim fiberboard

The reflection and transmission coefficients were measured separately from monostatic and bistatic tests with the same samples, ambient (water), and source/detectors (Fig. 8). The absorption coefficient was estimated based on calculating the remaining pulse energy from the emission source besides the reflection and transmission. Generally, all sample plates showed large acoustic absorption between 5 to 15 MHz. With different recipes and manufacturing, the acoustic energy separation behaved differently with an identical acoustic pulse source incidence. Both samples 15111 and 15121 had outstanding reflection coefficients. Samples 25111 and 25121 showed lower reflection coefficients. Sample 15111 transmitted a very limited amount of energy, where around 60% of energy was absorbed from 5 to 9 MHz and averaged 80% of the energy absorbed from 9 MHz to 15 MHz.

From 5 to 9 MHz, sample 15121 showed approximately 40% energy absorption and 80% absorption in the higher frequency range. For samples 25111 and 25121, the reflection coefficients showed less frequency dependence. The transmission and absorption coefficients behaved approximately proportionally, decreasing and increasing with the rise of the operating frequency. Sample 25121 showed maximum transmission in the lower frequency range due to higher density and compressibility. The testing results in this section showed great potential for the property engineering of denim fiberboard. Besides the commonly studied mechanical properties, the acoustic properties of the fiberboards can be artificially designed and modified by varying the recipe and manufacturing process to realize an acoustic resistor or damper.

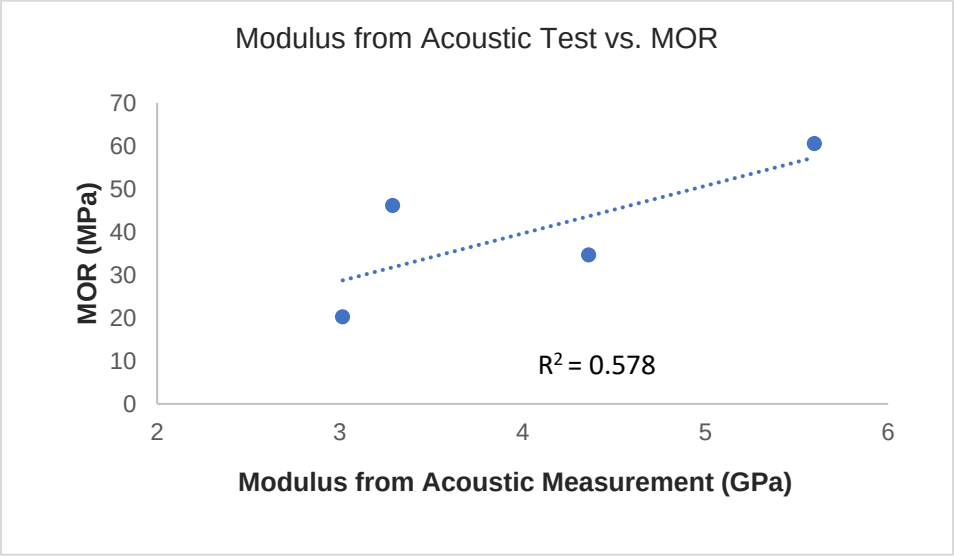

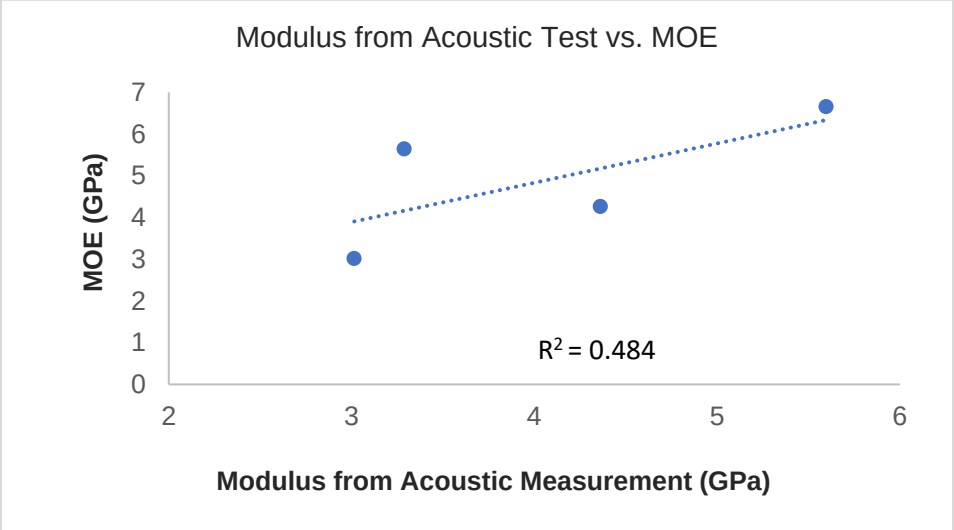

Fig. 9. Relationship between the modulus from the acoustic test and the bending properties

The moduli from the acoustic testing were similar to those tested MOEs, ranging between 3 to 6 GPa (Fig. 9). However, the correlation between the moduli from the EBME measurements and the MOE and MOR measured from the mechanical testing was not strong ($R^2 \sim 0.50$). The EBME technique measures the material's internal structure through the acoustic signals.

The modulus determined from EBME may not reflect the bending strength and modulus of the fiberboard directly. However, it would be more related to the internal bonding properties for the fiberboard. This was confirmed from the results on the relationship between the modulus from EBME and IB shown in Fig. 10. As shown in Fig. 10, A great correlation ($R^2 > 0.98$) was obtained between the modulus from EBME and the fiberboard's IB property. Therefore, the modulus determined from the EBME can be used as a good indicator for the IB, which is a critical property for the composites (Fig. 10).

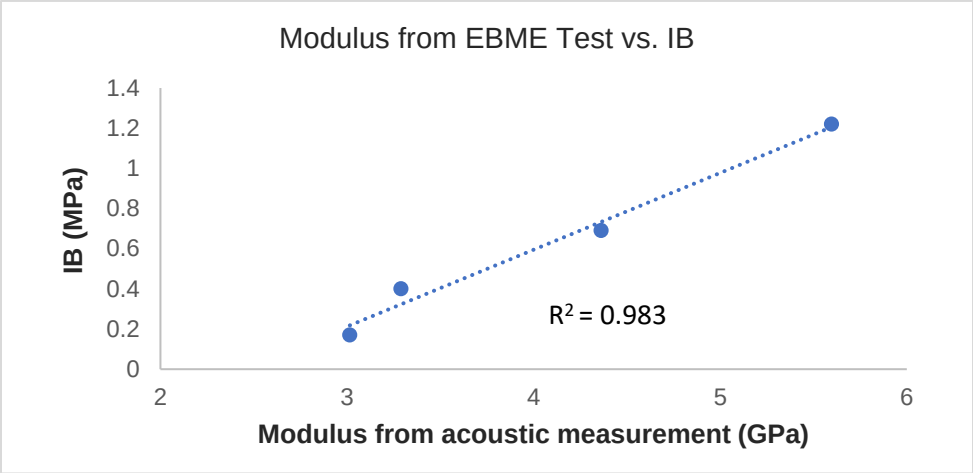

Fig. 10. Correlation between the modulus measured from acoustic testing and the internal bond

CONCLUSIONS

1. The denim fibers were successfully fabricated into the denim fiberboard. The internal bond strength (IB) of the denim fiberboard was significantly improved when more polymeric methylene diphenyl diisocyanate (pMDI) was used in the core of the board. It was shown that when using 17 wt% more pMDI in the core, the internal bond strength was enhanced by 306% for the 15% resin content and 205% for the 25% resin content. When 17 wt% more pMDI was used in the core of the fiberboard, the thickness swelling (TS) and water absorption (WA) after the 24-hour water emersion test were reduced by 60% and 69%, respectively at 15% resin content and 27% and 15% respectively at 25% resin content.
2. The effective bulk modulus elastography (EBME) technique is a great nondestructive tool for evaluating the internal structure of the composites. The modulus obtained from the EBME technique through the acoustic absorption and transmission measurements strongly correlated with the composites' internal bond properties. However, no specific correlations were found between the EBME modulus and bending properties of the fiberboard.
3. The EBME provides dynamic bulk modulus elastography, and the relative contrast in elasticity can be examined within the horizontal plane of the board. The elasticity distribution in the horizontal planes over each sample plate demonstrated the stability and compatibility between the composite recipes and manufacturing processes. The contrast in the slope and deviation in frequency dispersive phase velocity can be used to determine the uniformity in the vertical (thickness) direction, which was perpendicular to the layer structures on the sample plates with great variance in the acoustic absorption and transmission.

ACKNOWLEDGMENTS

The authors are grateful for the support of VF Jeanswear, Workwear, CASA, Greensboro, NC, USA.

REFERENCES CITED

Abolfazl, K., and Ahmad, J. L. (2011). "The performance of corn and cotton stalks for medium density fiberboard production," *BioResources* 6(2), 1147-1157. DOI: 10.15376/biores.6.2.11647-1157

Aghakhani, M., Enayati, S. H., Nadalizadeh, H., and Pirayesh, H. (2014). "The potential for using the sycamore (*Platanus orientalis*) leaves in manufacturing particleboard," *International Journal of Environmental Science and Technology* 11, 417-422. DOI: 10.1007/s13762-013-0327-8

ASTM D1037 (2020). "Standard test methods for evaluating properties of wood-base fiber and particle panel materials," ASTM International, West Conshohocken, PA.

ASTM D2395 (2017). "Standard test methods for density and specific gravity (relative density) of wood and wood-based materials," ASTM International, West Conshohocken, PA.

ASTM D4442 (2016). "Standard Test Methods for Direct Moisture Content Measurement of Wood and Wood-Based Materials," ASTM International, West Conshohocken, PA.

Batiancela, M. A. (2014). "Particleboard from waste tea leaves and wood particles," *Journal of Composite Materials* 48(8), 911-916. DOI: 10.1177/0021998313480

Bhuiyan, M. Y., Bao, J., Poddar, J. B., and Giurgiutiu, V. (2018). "Toward identifying crack-length-related resonances in acoustic emission waveforms for structural health monitoring applications," *Structural Health Monitoring* 17(3), 577-585. DOI: 10.1177/147592171770735

Boni, E, Alfred, C. H., Freear, S., Jensen J. A., and Tortoli, P. (2018). "Ultrasound open platforms for next-generation imaging technique development," *IEEE Transactions on Ultrasonics, Ferroelectrics, and Frequency Control* 65(7), 1078-1092. DOI: 10.1109/TUFFC.2018.2844560

Cheng, X., He, X., Xie, J., Quan, P., Xu, K., Li X., and Cai, Z. (2016). "Effect of the particle geometry and adhesive mass percentage on the physical and mechanical properties of particleboard made from peanut hull," *BioResources* 11(3), 7271-7281.

Ferrández-García, C. (2018). "Physical and mechanical properties of particleboard made from palm tree prunings," *Forests* 9, 755; DOI:10.3390/f9120755, 2018

Gonçalves, R., Trinca, A. J., and Cerri, D. G. P. (2011). "Comparison of elastic constants of wood determined by ultrasonic wave propagation and static compression testing," *Wood and Fiber Science* 43(1), 64-75.

Hsu, D. K., Utrata, D., and Kuo, M. (2010, February). "NDE of lumber and natural fiber based products with air coupled ultrasound," in: *AIP Conference Proceedings* (Vol. 1211, No. 1, pp. 1533-1540). American Institute of Physics.

Hwang, Y. I., Park, J., Kim, H. J., Song, S. J., Cho, Y. S., and Kang, S. S. (2019). "Performance comparison of ultrasonic focusing techniques for phased array ultrasonic inspection of dissimilar metal welds," *International Journal of Precision Engineering and Manufacturing* 20(4), 525-534. DOI: 10.1007/s12541-019-00085-1

Iswanto, A. H., Azhar, I., and Susilowati, A. S. (2014). "Effect of resin type, pressing temperature and time on particleboard properties made from sorghum bagasse," *Agric. For. Fish*. 3(2), 62-66. DOI: 10.11648/j.aff.20140302.12

Jin, Y., Walker, E., Krokhin, A., Heo, H., Choi, T. Y., and Neogi, A. (2019). "Enhanced instantaneous elastography in tissues and hard materials using bulk modulus and density determined without externally applied material deformation," *IEEE*

Transactions on Ultrasonics, Ferroelectrics, and Frequency Control 67(3), 624-634.
Jin, Y., Walker, E., Heo, H., Krokhin, A., Choi, T. Y., and Neogi, A. (2020a). "Non-destructive ultrasonic evaluation of fused deposition modeling based additively manufactured 3D-printed structures," *Smart Materials and Structures* 29(4), article 045020.
Jin, Y., Yang, T., Heo, H., Krokhin, A., Shi, S. Q., Dahotre, N., Choi, T. Y., and Neogi, A. (2020b). "Novel 2D dynamic elasticity maps for inspection of anisotropic properties in fused deposition modeling objects," *Polymers* 12(9), 1966.
Jin, Y., Heo, H., Walker, E., Krokhin, A., Choi, T. Y., and Neogi, A. (2020c). "The effects of temperature and frequency dispersion on sound speed in bulk poly (vinyl alcohol) poly (N-isopropyl acrylamide) hydrogels caused by the phase transition," *Ultrasonics* 104, article 105931.
Legendre, S., Goyette, J., and Massicott, D. (2001). "Ultrasonic NDE of composite material structures using wavelet coefficients," *NDT and E Internat.* 34(1), 31-37. DOI: 10.1016/S0963-8695(00)00029-3
Lewin, M. (2006). *Handbook of Fiber Chemistry*, CRC Press, Boca Raton, FL, USA. DOI: 10.1201/9781420015270
Li, X., Wang, S., Du, G., Wu, Z., and Gong, Y. (2014). "Manufacturing particleboard using hemp shiv and wood particles with low free formaldehyde emission urea-formaldehyde resin," *Forest Products Journal* 64 (5-6), 187-191.
Li, Y., Zhang, Y., Dong, W., Yue, J., Xu, M., and Shi, S. Q. (2018). "Preparation and properties of pulp fibers treated with zinc oxide nanoparticles by in situ chemosynthesis," *Holzforschung* 72(11), 923-931. DOI: 10.1515/hf-2018-0013
Luiken, A., and Bouwhuis, G. (2015). "Recovery and recycling of denim waste," in: *Denim: Manufacturing, Finishing and Application*, Woodhead Publishing Series in Textiles, pp. 527-540. DOI: 10.1016/B978-0-85709-843-6.00018-4
McLoughlin, J., Hayes, S., and Paul, R. (2015). "Cotton fibre for denim manufacture," in: *Denim: Manufacturing, Finishing and Application*, Woodhead Publishing Series in Textiles, Elsevier, New York, pp. 15-36. DOI: 10.1016/B978-0-85709-843-6.00002-0
Minh, H. N., Du, J., and Raum, K. (2019). "Estimation of thickness and speed of sound in cortical bone using multifocus pulse-echo ultrasound," *IEEE Transactions on Ultrasonics, Ferroelectrics, and Frequency Control* 67(3), 568-579. DOI: 10.1109/TUFFC.2019.2948896
Mohebby, B., Iibeighi, F., and Kazemi-Najafi, S. (2008). "Influence of hydrothermal modification of fibers on some physical and mechanical properties of medium density fiberboard (MDF)," *Holz Roh Werkst*. 66, 213-218. DOI 10.1007/s00107-008-0231-y.
Nath, D. C., and Mwchahary, D. D. (2012). "Population Increase and deforestation: A study in Kokrajhar Distric of Assam," *India. Int. J. Sci. Res. Publ*. 20(2), 1-12.
Ndazi, B., Tesha, J.V., and Bisanda, E. T. N. (2006). "Some opportunities and challenges of producing bio-composites from non-wood residues," *J. Mater. Sci*. 41(2006), 6984-6990. DOI: 10.1007/s10853-006-0216-3
Neogi, A., Walker, E., and Jin, Y. (2020). "Non-destructive ultrasonic elastographic imaging for evaluation of materials," World. Patent WO2020242994A1, 03 12 2020.
Pantawane, M. V., Yang, T., Jin, Y., Joshi, S. S., Dasari, S., Sharma, A., Krokhin, A., and Al, E. (2021). "Crystallographic texture dependent bulk anisotropic elastic response of additively manufactured Ti6Al4V," *Scientific Reports* 11(1), 1-10. DOI: 10.1038/s41598-020-80710-6
Pirayesh, H., Khazaeian, A., and Tabarsa, T. (2012). "The potential for using walnut

(*Juglans regia* L.) shell as a raw material for wood-based particleboard manufacturing," *Composites Part B*. 43(8), 3276-3280. DOI: 10.1016/j.compositesb.2012.02.016

Reese, S. J., Smith, D. S., Rupp, R. E., Wright, J. K., Khanolkar, A. R., Wright, R. N., and Hurley, D. H. (2021). "Elevated-temperature elastic properties of alloys 709 and 617 measured by laser ultrasound," *Journal of Materials Engineering and Performance* 30(2), 1513-1520.

Sandoz, J. L. (1993). "Moisture content and temperature effect on ultrasound timber grading," *Wood Science and Technology* 27(5), 373-380.

Sarro, W. S., and Ferreira, G. C. S. (2019). "Soil elastic modulus determined by ultrasound tests," *Soils and Rocks* 42(2), 117-126. DOI: 10.28927/SR.422117

Sfarra, S., Theodorakeas, P., Avdelidis, N. P., and Koui, M. (2013). "Thermographic, ultrasonic and optical methods: A new dimension in veneered wood diagnostics," *Russian Journal of Nondestructive Testing* 49(4), 234-250.

Sigrist, R. M., Liau, J., Kaffas, A. E., Chammas, M. C., and Willmann, J. K. (2017). "Ultrasound elastography: Review of techniques and clinical applications," *Theranostics* 7(50), 1303.

Smith, L. M., and Shi, S. Q. (2015). "Hygroscopic properties of kenaf bast fiber reinforced epoxy resin composites fabricated from vacuum assisted resin transfer molding process," *Journal of Chemical Engineering and Chemistry Research* 2(9).

Taheri, H., and Hassen, A. A. (2019). "Non-destructive ultrasonic inspection of composite materials: A comparative advantage of phased array ultrasonic," *Applied Sciences* 9(8), 1628. DOI: 10.3390/app9081628

Tang, H., Qu, X., and Yue, B. (2019). "Diagnostic test accuracy of magnetic resonance imaging and ultrasound for detecting bone erosion in patients with rheumatoid arthritis," *Clinical Rheumatology* 39(4), 1283-1293. DOI: 10.1007/s10067-019-04825-6

Temitope, A. K., Onaopemipo, A. T., Olawale, A. A., and Abayomi, O. O. (2015). "Recycling of rice husk into a locally-made water-resistant particle board," *Ind. Eng. Manage.* 4(3), article 1000164. DOI: 10.4172/2169-0316.1000164

United States Environmental Protection Agency. (2016). Advancing Sustainable Materials Management: 2014 Fact Sheet

Vun, R. Y., Wu, Q., and Monlezun, C. J. (2003). "Ultrasonic characterization of horizontal density variations in oriented strandboard," *Wood and Fiber Science* 35(4), 482-498.

Wakelyn, P. J., Bertoniere, N. R., French, A. D. Thibodeaux, D. P., Triplett, B. A., Rousselle, M., Goynes Jr., W. R., Edwards, V., Hunter, L., McAlister, D. D., and Gamble, G. R. (2006). *Cotton Fiber Chemistry and Technology*, Taylor & Francis Group, Boca Raton, CRC Press.

Wang, C., Wang, G., Cheng, H., Zhang, S., Smith, L. M., and Shi, S. Q. (2017). "$CaCO_3$ *in situ* treated bamboo pulp fiber reinforced composites obtained by vacuum-assisted resin infusion," *Wood Science and Technology* 51, 571-584. DOI: 10.1007/s00226-017-0900-2

Wang, Q., Xiao, S., and Shi, S. Q. (2020). "Natural fiber-metallic composites with remarkable gradient structure," *Materials Today Communications* 25, article 101453. DOI: 10.1016/j.mtcomm.2020.101453

Xia, C., Shi, S. Q., and Cai, L. (2015). "Vacuum-assisted resin infusion (VARI) and hot pressing for $CaCO_3$ nanoparticle treated kenaf fiber reinforced composites," *Composites Part B*. 78, 138-143. DOI: 10.1016/j.compositesb.2015.03.039

Yang, H., and Yu, L. (2017). "Feature extraction of wood-hole defects using wavelet-based ultrasonic testing," *Journal of Forestry Research* 28(2), 395-402. DOI: 10.1007/s11676-016-0297-z

Article submitted: December 8, 2022; Peer review completed: January 14, 2023; Revised version received and accepted: January 31, 2023; Published: March 20, 2023.
DOI: 10.15376/biores.18.2.3279-3294